THE JOURNAL OF BIOLOGICAL CHEMISTRY VOL. 283, NO. 25, pp. 17065–17074, June 20, 2008
© 2008 by The American Society for Biochemistry and Molecular Biology, Inc. Printed in the U.S.A.

Structural and Biochemical Properties of Lipid Particles from the Yeast *Saccharomyces cerevisiae*[*]

Received for publication, January 16, 2008, and in revised form, April 14, 2008 Published, JBC Papers in Press, April 22, 2008, DOI 10.1074/jbc.M800401200

Tibor Czabany[‡1], Andrea Wagner[‡1], Dagmar Zweytick[§], Karl Lohner[§], Erich Leitner[¶], Elisabeth Ingolic[‖], and Günther Daum[‡2]

From the [‡]Institute of Biochemistry, Graz University of Technology, Petersgasse 12, A-8010 Graz, [§]Institute of Biophysics and Nanosystems Research, Austrian Academy of Sciences, Schmiedlstrasse 6, A-8042 Graz, [¶]Institute for Food Chemistry and Technology, Graz University of Technology, Petersgasse 12, A-8010 Graz, and [‖]Research Institute for Electron Microscopy and Finestructure Research, Graz University of Technology, Steyrergasse 17/III, A-8010 Graz, Austria

The two most prominent neutral lipids of the yeast *Saccharomyces cerevisiae*, triacylglycerols (TAG) and steryl esters (SE), are synthesized by the two TAG synthases Dga1p and Lro1p and the two SE synthases Are1p and Are2p. In this study, we made use of a set of triple mutants with only one of these acyltransferases active to elucidate the contribution of each single enzyme to lipid particle (LP)/droplet formation. Depending on the remaining acyltransferases, LP from triple mutants contained only TAG or SE, respectively, with specific patterns of fatty acids and sterols. Biophysical investigations, however, revealed that individual neutral lipids strongly affected the internal structure of LP. SE form several ordered shells below the surface phospholipid monolayer of LP, whereas TAG are more or less randomly packed in the center of the LP. We propose that this structural arrangement of neutral lipids in LP may be important for their physiological role especially with respect to mobilization of TAG and SE reserves.

Fatty acids and sterols are important building blocks of biomembranes. To maintain balanced cellular levels of these components, a certain portion is put on hold in the form of complex neutral lipids. The yeast *Saccharomyces cerevisiae* similar to other eukaryotic cells stores fatty acids and sterols in the form of triacylglycerols (TAG)[3] and steryl esters (SE). Both TAG and SE are hydrophobic molecules that are not soluble in the cytosol but are also not typical bilayer membrane lipids. Consequently, they need to be stored in specific subcellular compartments that are known as lipid particles (LP), lipid droplets, lipid bodies, or oil bodies. Yeast LP are small spherical organelles with an approximate diameter of 400 nm consisting of 95% neutral lipids, TAG, and SE, and only small amounts of phospholipids and proteins (1). The highly hydrophobic core formed by TAG and SE is surrounded by a phospholipid monolayer containing a well defined set of proteins (2).

Identification of LP proteins in various types of cells has changed the view of this organelle. The presence of certain enzymes on the surface of LP suggests that besides lipid storage LP are involved in various metabolic processes. In *S. cerevisiae* ~40 proteins are known to be present on the surface of LP. Strikingly, most of these proteins are enzymes involved in lipid metabolism. As prominent examples, LP from *S. cerevisiae* harbor enzymes of phosphatidic acid biosynthesis (3), fatty acid activation (4–6), sterol biosynthesis (7), but also TAG biosynthesis and degradation (8–11) and SE hydrolysis (12–14).

The biogenesis of LP is still a matter of dispute and is under investigation in several laboratories. Whereas little is known about the cell biology of this process, enzymes involved in the formation of major LP components, TAG and SE, have been identified within the last few years (for recent review see Refs. 15 and 16). In the yeast as in other types of cells, the last step of TAG synthesis requires acylation of diacylglycerol. Two different mechanisms of TAG synthesis have been demonstrated in *S. cerevisiae*. First, the acyl-CoA-independent acyltransferase Lro1p was identified. This enzyme requires phospholipids as an acyl donor (17, 18) and combines functions of a phospholipase A_2 (or B) and an acyltransferase. Lro1p appears to be exclusively localized to the endoplasmic reticulum (ER). The other enzyme involved in TAG synthesis is Dga1p, which is an acyl-CoA-dependent acyltransferase. Under standard growth conditions, Dga1p appears to be more active than Lro1p (9). In the yeast, Dga1p is dually localized to the ER and LP. The TAG synthase activity of Dga1p on LP demonstrated *in vitro* (19) may be responsible for the formation of TAG directly at its site of storage.

SE of *S. cerevisiae* are synthesized by two closely related sterol acyltransferases named Are1p and Are2p (20, 21). Both enzymes are localized to the ER and utilize acyl-CoA as acyl donor (7), but they differ in regulation and substrate specificity as shown by experiments with single or double deletion strains. Are2p includes most of the acyl-CoA:sterol acyltransferase activity in the yeast and esterifies preferentially ergosterol, the final product of sterol synthesis in the yeast (20, 22–24). Interestingly, Are1p was shown to exhibit increased activity under

* This work was supported by the Fonds zur Förderung der Wissenschaftlichen Forschung in Österreich Projects 18857 and W901-B05 (to G. D.). The costs of publication of this article were defrayed in part by the payment of page charges. This article must therefore be hereby marked "*advertisement*" in accordance with 18 U.S.C. Section 1734 solely to indicate this fact.

[1] Both authors contributed equally to this work.

[2] To whom correspondence should be addressed: Institute of Biochemistry, Graz University of Technology, Petersgasse 12/II, A-8010 Graz, Austria. Tel.: 43-316-873-6462; Fax: 43-316-873-6952; E-mail: guenther.daum@tugraz.at.

[3] The abbreviations used are: TAG, triacylglycerol; CE, cholesteryl ester; ER, endoplasmic reticulum; LP, lipid particle; PL, phospholipid; SE, steryl ester; CHAPS, 3-[(3-cholamidopropyl)dimethylammonio]-1-propanesulfonic acid; MES, 4-morpholineethanesulfonic acid; CER, cholesterol-rich; LDL, low density lipoprotein; VLDL, very LDL; TM, triple mutant; GLC, gas-liquid chromatography; MS, mass spectrometry; DSC, differential scanning calorimetry; SAXS, small angle x-ray scattering.

This is an Open Access article under the CC BY license.

hypoxic conditions and to prefer sterol precursors as substrates. The presence of two SE synthases with overlapping function, which are subject to differential regulation, might reflect the different roles of these enzymes in sterol homeostasis under optimal or suboptimal conditions of ergosterol biosynthesis. Screening for yeast mutants that were nonviable in the absence of sterol esterification led to the identification of *ARV1* (25). Besides their dependence on sterol esterification for growth, *arv1*Δ deletion strains were nystatin-sensitive, temperature-sensitive, and nonviable under anaerobic conditions. Cells lacking Arv1p also displayed an altered intracellular sterol distribution and were defective in sterol uptake, consistent with a possible role for Arv1p in sterol trafficking to the plasma membrane.

LP as a storage compartment would be useless without enzymes that mobilize the lipid depots, especially fatty acids and sterols from TAG or SE. In *S. cerevisiae*, three TAG lipases and two SE hydrolases present on the surface of LP were identified (10–14). The major TAG lipase of *S. cerevisiae* identified at the molecular level and by function is Tgl3p (10). Based on homology to Tgl3p, two additional TAG lipases, Tgl4p and Tgl5p, were also identified. Similar to Tgl3p, Tgl4p and Tgl5p are involved in TAG catabolism *in vivo*, exhibit enzymatic activity *in vitro* when purified close to homogeneity, and localize to LP close to their substrate (11, 26).

Recently, three SE hydrolases of the yeast *S. cerevisiae* were identified. The highest SE hydrolase activity present in the plasma membrane (7) was attributed to Yeh2p (12, 13). The physiological role of this SE hydrolase in the plasma membrane is still a matter of dispute. In contrast, two other members of the yeast SE hydrolase family, Yeh1p and Tgl1p, were localized to LP (13, 14). These two enzymes exhibited a very low activity *in vitro*, but a triple deletion in combination with *YEH2* completely abolished SE hydrolysis in the yeast. In an *hem1*Δ deletion strain mimicking anaerobic growth, Yeh1p became the most important SE hydrolase, whereas Yeh2p and Tgl1p were largely inactive under this condition (27).

Despite the progress that has been made during the last few years to identify gene products involved in neutral lipid metabolism, the biogenesis of the neutral lipid storage compartment, the LP, is still poorly understood. A rather fundamental although highly important question related to this problem is coordination of the different enzyme activities contributing to biosynthesis and degradation of neutral lipids. To address this question from the viewpoint of LP formation, we studied the contribution of individual TAG and SE synthases to this process. For this purpose, we employed triple mutants (TM) with only one of the four acyltransferases active, Dga1p, Lro1p, Are1p, or Are2p, respectively. This strategy led us to investigate the following: (i) the influence of neutral lipid-synthesizing steps between each other and other lipid-forming processes, *e.g.* sterol synthesis; and (ii) the structure of LP variants with unusual but well defined neutral lipid composition. The result of this study is a novel model of yeast LP structure presented here, which is based on biochemical and biophysical properties of this organelle.

EXPERIMENTAL PROCEDURES

Strains, Culture Conditions, and Subcellular Fractionation—Yeast strains used throughout this study are listed in the Table 1. Cells were grown aerobically to the late logarithmic (16 h) or stationary phase (24 h) at 30 °C in YPD medium containing 1% yeast extract (Oxoid), 2% peptone (Oxoid), and 2% glucose (Merck). Media were inoculated with precultures grown aerobically for 24 h in YPD medium at 30 °C to an A_{600} of 0.1.

The yeast lipid particle (LP) fraction was obtained at high purity from cells grown to the early stationary phase as described by Leber *et al.* (1). The isolation of other subcellular fractions used in this study was described by Zinser and Daum (28). The quality of subcellular fractions was routinely tested by Western blot analysis (see below).

Protein Analysis—Proteins were quantified by the method of Lowry *et al.* (29) using bovine serum albumin as a standard. Proteins were precipitated with trichloroacetic acid and solubilized in 0.1% SDS, 0.1 M NaOH prior to quantification. When LP fractions were analyzed, samples were delipidated prior to protein quantification. For this purpose, nonpolar lipids were extracted with 2 volumes of diethyl ether, and the organic phase was withdrawn; residual diethyl ether was removed under a stream of nitrogen, and proteins were precipitated as described above.

SDS-PAGE was carried out by the method of Laemmli (30) using 10% SDS gels. Samples were denaturated at 37 °C to avoid hydrolysis of polypeptides. Proteins on gels were detected by staining with Coomassie Blue. Western blot analysis was performed according to Haid and Suissa (31). All primary antibodies used in this study were from rabbits and were directed against Erg1p, Por1p, Wbp1p, and Prc1p/CPY. Peroxidase-conjugated secondary antibody and enhanced chemiluminescent signal detection reagents (SuperSignal™, Pierce) were used to visualize immunoreactive bands.

Lipid Extraction and Analysis—Lipids from yeast cells were extracted as described by Folch *et al.* (32). For quantification of neutral lipids, extracts were applied to Silica Gel 60 plates with the aid of a sample applicator (CAMAG, Automatic TLC Sampler 4, Muttenz, Switzerland), and chromatograms were developed in an ascending manner by a two-step developing system. First, light petroleum:diethyl ether:acetic acid (25:25:1; per volume) was used as mobile phase, and plates were developed to half-distance of the plate. Then the plates were dried briefly and further developed to the top of the plate using the second mobile phase consisting of light petroleum:diethyl ether (49:1; v/v). To visualize separated bands, TLC plates were dipped into a charring solution consisting of 0.63 g of $MnCl_2 \cdot 4H_2O$, 60 ml of water, 60 ml of methanol, and 4 ml of concentrated sulfuric acid, briefly dried, and heated at 100 °C for 30 min. The lipids were then quantified by densitometric scanning at 400 nm using a Shimadzu dual-wave length chromatoscanner CS-930 with triolein and cholesteryl ester as standards.

Fatty acids were analyzed by gas-liquid chromatography (GLC). Lipid extracts prepared as described above were subjected to methanolysis using BF_3/methanol and converted to methyl esters as described by Morrison and Smith (33). Fatty acid methyl esters were separated using a Hewlett-Packard

6890 gas chromatograph equipped with an HP-INNOWax capillary column (15 m × 0.25 mm inner diameter × 0.50 μm film thickness) and helium as carrier gas. Fatty acids were identified by comparison to commercial fatty acid methyl ester standards (NuCheck, Inc., Elysian, MN).

Individual sterols from whole cells or LP were identified and quantified by GLC/mass spectrometry (MS) after alkaline hydrolysis of lipid extracts (34). GLC/MS was performed on a Hewlett-Packard 5890 gas chromatograph equipped with a mass selective detector (HP 5972), using an HP5-MS capillary column (30 m × 0.25 mm × 0.25 μm film thickness). Aliquots of 1 μl were injected in the splitless mode at 270 °C injection temperature with helium as a carrier gas at a flow rate of 0.9 ml/min in constant flow mode. The following temperature program was used: 1 min at 100 °C, 10 °C/min to 250 °C, and 3 °C/min to 310 °C. Mass spectra were acquired in scan mode (scan range 200–550 atomic mass units) with 3.27 scans/s. Sterols were identified based on their mass fragmentation pattern.

Enzymatic Assays—For the preparation of [^{14}C]palmitic acid-labeled phospholipids, cells were inoculated to an A_{600} of 0.5 in 100 ml of minimal media containing 520 nmol (30 μCi) of [^{14}C]palmitic acid (PerkinElmer Life Sciences) and incubated for 4 h at 30 °C. The cells were then harvested, and lipids were extracted and separated as described above. The phospholipid fraction was extracted from TLC plates into 1 ml of chloroform:methanol (2:1, v/v), and radioactivity was measured by liquid scintillation counting using LSC safety mixture (Baker, Deventer, The Netherlands) and 5% water as a scintillation mixture.

The acyl-CoA:diacylglycerol acyltransferase assay was performed in a final volume of 100 μl containing 6 nmol of [^{14}C]oleoyl-CoA (80,000 dpm), 0.025 mM dioleoylglycerol, 0.5 mM CHAPS, 150 mM Tris-Cl (pH 7.0), 15 mM KCl, 15 mM $MgCl_2$, and 100 μg of yeast cell homogenate (19). The phospholipid:diacylglycerol acyltransferase assay was performed in the final volume of 100 μl containing [^{14}C]palmitic acid-labeled phospholipids (70,000 dpm, 188 nmol), 0.05 mM dioleoylglycerol, 150 mM Tris-Cl (pH 7.0), 15 mM KCl, 15 mM $MgCl_2$, and 200 μg of protein (18). The acyl-CoA:ergosterol acyltransferase assay was performed in the final volume of 100 μl containing 6 nmol of [^{14}C]oleoyl-CoA (80,000 dpm), 0.025 mM ergosterol, 0.5 mM CHAPS, 100 mM KH_2PO_4 (pH 7.4), 1 mM dithiothreitol, and 100 μg of protein (35).

Incubations were carried out for 20 or 30 min at 30 °C and terminated by addition of 300 μl of chloroform:methanol (2:1, v/v). Lipids were extracted twice for 10 min with shaking using 300 μl of chloroform:methanol (2:1, v/v). Organic phases were combined and washed twice using methanol:water:chloroform (47:48:3; per volume). The organic phase was taken to dryness under a stream of nitrogen. Lipids were dissolved in 30 μl of chloroform:methanol (2:1, v/v), separated by TLC as described above, and visualized on TLC plates by staining with iodine vapor. Bands were scraped off, and radioactivity was measured by liquid scintillation counting using LSC safety mixture (Baker, Deventer, The Netherlands) and 5% water as a scintillation mixture.

Electron Microscopy of Whole Yeast Cells—Yeast cells grown on YPD were sedimented by centrifugation, rinsed in 0.1 M cacodylate buffer (pH 7.4), and fixed with 3% glutaraldehyde in 0.1 M cacodylate buffer (pH 7.4) containing 5 mM $CaCl_2$ and 5 mM $MgCl_2$ for 3 h at room temperature and 3 h on ice. The cells were then washed twice with 0.1 M cacodylate buffer (pH 7.4) and postfixed in 4% $KMnO_4$, prepared in distilled H_2O for 90 min. After rinsing the pellet four times, cells were treated with 0.5% sodium metaperiodate for 15 min at room temperature, washed once more with distilled H_2O, and dispersed in a 2% agarose solution (1:1). The solidified agar containing the cells was cut into small cubes of about 1 mm^3 and placed into 2% uranyl acetate in distilled H_2O for *en bloc* staining overnight on ice. Blocks were washed with distilled H_2O and dehydrated through a graded series of acetone, 10 min each, followed by three washes with 100% acetone for 15 min each. Samples were incubated in 2:1, 1:1, and 1:2 mixtures of acetone/Spurr resin for 2 h, respectively. The last incubation step was performed overnight to allow slow evaporation of acetone. After removal of the Spurr resin, agar cubes were incubated in fresh 100% Spurr resin for another 2 h. The samples were then placed into gelatin capsules containing fresh Spurr resin (100%), and capsules were placed in a polymerization oven at 70 °C for 48 h (12). Using a diamond knife (Diatome), 75-nm ultrathin sections were cut on a Leica Ultracut E ultramicrotome and collected into 75 mesh copper palladium grids with a support film of pioloform. Sections were stained in 1% uranyl acetate in distilled H_2O for 20 min, washed, and stained once more in lead citrate (36). Images were produced on a Tecnai G^2 12 (FEI Co.) equipped with a CCD camera (Gatan Bioscan) at 100 kV.

Differential Scanning Calorimetry (DSC)—Calorimetric experiments were performed with a differential scanning calorimeter (VP-DSC) from MicroCal, Inc., Northampton, MA. Samples of LP prepared from wild type and mutant strains were used undiluted. A buffer containing 0.25 M sorbitol, 10 mM MES/Tris, and 0.2 mM Na_2EDTA (pH 6.9) was used to fill the reference cell, and samples were degassed before measuring. Heating scans were performed at a scan rate of 15 °C/h between 1 and 65 °C. Pre-scan thermostating was allowed for 60 min. Enthalpies were calculated by integrating the peak area after base-line adjustment and normalization to SE concentrations using the MicroCal Origin software (VP-DSC version).

SAXS—X-ray diffractograms were recorded with a SWAX-camera (HECUS x-ray Systems, Graz, Austria) that was mounted on a sealed tube Seifert generator (Ahrensburg, Germany) operating at 2 kilowatts (50 kV and 40 mA). The x-ray beam was filtered for CuK_α-radiation ($\lambda = 1.54$ Å) using a nickel foil and a pulse-height discriminator built into the detection system. The scattered intensity was recorded with two linear position-sensitive detectors (PSD 50, HECUS X-ray Systems, Graz, Austria) simultaneously in the small angle regimes of 10^{-3} Å$^{-1} < q < 1$ Å^{-1} (SAXS), where $q = 4\pi \sin(\theta)/\lambda$ is the modulus of the scattering wave vector. Calibration was performed with silver stearate. Samples of LP prepared from yeast wild type and mutant strains were loaded into thin walled quartz capillaries thermally equilibrated for 60 min at 1 °C before initiating data acquisition. Temperature was controlled with an accuracy of 0.1 °C with

TABLE 1
Yeast strains used in this study

Strain	Relevant genotype	Source of Ref.
W303 (wild type)	*SUC2 GAL$^+$ mal mel ade2-1 can1-100 his3-11,15 leu2-3 112 trp1-1 ura3-1*	ScanBi Ltd., Alnarp, Sweden (37)
TM *DGA1$^+$*	*W303; MATα lro1::TRP1 are1::HIS3 are2::LEU2 ADE2 met ura3*	ScanBi Ltd., Alnarp, Sweden
TM *LRO1$^+$*	*W303; MATα dga1::KanMX4 are1::HIS3 are2::LEU2 ADE2 met trp1 ura3*	ScanBi Ltd., Alnarp, Sweden
TM *ARE1$^+$*	*W303; MATα dga1::KanMX4 lro1::TRP1 are2::LEU2 ADE2 met his3 ura3*	ScanBi Ltd., Alnarp, Sweden
TM *ARE2$^+$*	*W303; MATα dga1::KanMX4 lro1::TRP1 are1::HIS3 ADE2 met leu2 ura3*	ScanBi Ltd., Alnarp, Sweden
QM[a]	*W303; MATα dga1::KanMX4 lro1::TRP1 are1::HIS3 are2::LEU2 ADE2 met ura3*	ScanBi Ltd., Alnarp, Sweden

[a] QM indicates quadruple mutant.

a programmable Peltier unit. Diffraction patterns were recorded at each temperature for 7200 s. Measurements were performed at 1, 35, and 65 °C.

Zetasizer Measurements—Dynamic light scattering was used to determine the mean diameter and size distribution of LP from yeast wild type and mutant strains using a Zetasizer 3000HS (Malvern Instruments, Worcestershire, UK). The instrument was equipped with a 10-milliwatt helium-neon laser operating at a wavelength of 632.8 nm. The scattered light was detected at an angle of 90° by a photon-counting avalanche photodiode detector coupled to the correlator. Particle size calculation was derived from an autocorrelation function. For measurements, samples were diluted with water that was filtered (pore size 0.02 μm) prior to use to avoid dust particles interfering with measurements. To check reproducibility, a series of three measurements were performed at room temperature.

RESULTS

S. cerevisiae produces TAG and SE by catalysis of four acyltransferases, Dga1p, Lro1p, Are1p, and Are2p. To address the question as to the role of individual enzymes to the formation of neutral lipids and thus to the biogenesis of LP, we used triple mutants (TM) with only one of the four acyltransferases active as an experimental system. LP from the different TM were isolated at highest purity and subjected to various biochemical, cell biological, and biophysical analyses.

Neutral Lipids of Triple Mutants—Neutral lipids of the yeast start accumulating at the end of the logarithmic phase and reach a high level in the stationary phase when cells stop dividing. Therefore, the correct time point of harvesting was important to compare the amounts of neutral lipids from wild type and TM. Because wild type and TM used in this study (Table 1) grow similarly on YPD (data not shown), TAG and SE were quantified from cells grown to the late logarithmic (16 h) and mid-stationary phase (24 h). As can be seen from Fig. 1*A*, the amount of TAG from wild type W303 increased approximately three times between the two time points taken. A TM with only Lro1p active (TM *LRO1$^+$*) showed a marked decrease of the TAG amount compared with wild type after 16 or 24 h of growth, respectively. However, the level of TAG was also increased in this strain from the late logarithmic to the mid-stationary phase, although it had been argued before that Lrop1p in contrast to Dga1p was more active in logarithmic phase (9). A triple mutant with Dga1p as the only active acyltransferase (TM *DGA1$^+$*) exhibited a TAG level that was similar to wild type, showing a similar increase in the TAG level from 16 to 24 h of growth. Dga1p had been assumed to remain active within the stationary phase (9). It

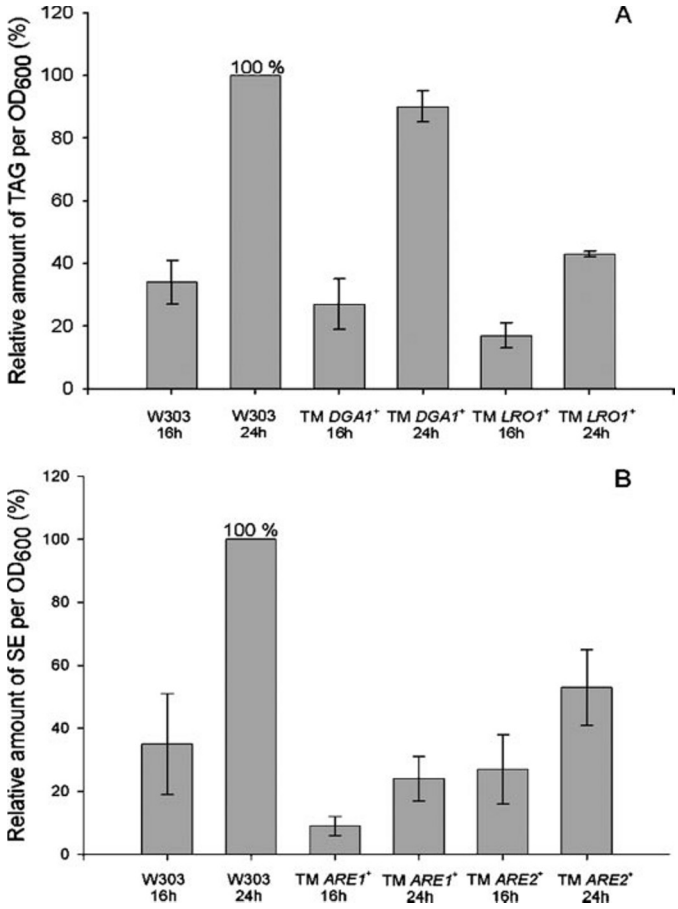


FIGURE 1. **Neutral lipid composition of wild type and triple mutants with only one active acyltransferase from cells grown to the late logarithmic (16 h) and stationary (24 h) phase.** Data are mean values of four independent experiments. The amounts of TAG and SE per A_{600} found in the wild type after 24 h were set at 100%. *A,* relative amount of TAG from wild type, TM *DGA1$^+$*, and TM *LRO1$^+$*. *B,* relative amount of SE from wild type, TM *ARE1$^+$*, and TM *ARE2$^+$*.

has to be mentioned that neither TM *DGA1$^+$* nor TM *LRO1$^+$* contained SE.

TM with only Are1p or Are2p active (TM *ARE1$^+$* and TM *ARE2$^+$*) form SE as the major neutral lipid components (Fig. 1*B*). Using sensitive radiolabeling techniques, it had been shown before that Are1p and Are2p are able to synthesize also minor amounts of TAG (9, 37). In our experiments, however, TAG was not detectable in these strains because of the less sensitive analytical method employed in this study. In the wild type, the amount of SE is increased by 60% from 16 to 24 h of growth. This enhancement appears to be attributable to both Are1p and Are2p, because SE in TM *ARE1$^+$* and TM *ARE2$^+$* increased accordingly over the observed time period. The con-

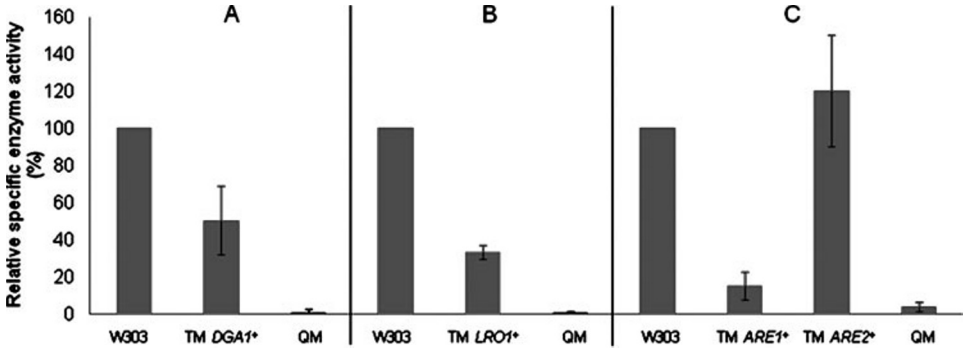


FIGURE 2. **Activities of neutral lipid-synthesizing enzymes *in vitro*.** Activity was measured *in vitro* using cell homogenates for acyl-CoA:diacylglycerol acyltransferase (*A*) and acyl-CoA:ergosterol acyltransferase (*C*). Phospholipid:diacylglycerol acyltransferase (*B*) was measured using crude ER fractions. Strains are described in Table 1. Data are from three independent experiments. The specific activity of each enzyme in wild type was set as 100%. The quadruple mutant (*QM*) *dga1*Δ*lro1*Δ*are1*Δ*are2*Δ was used as negative control.

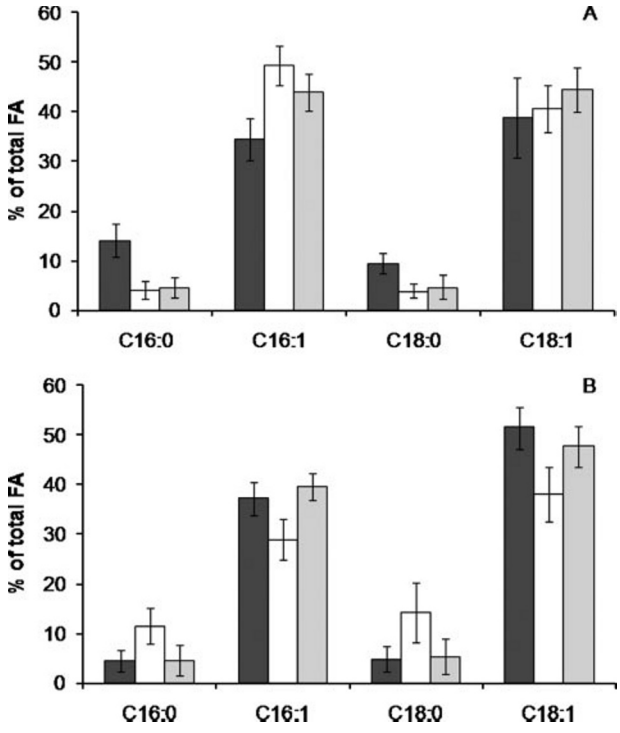


FIGURE 3. **Fatty acid analysis of neutral lipids.** *A,* fatty acid analysis of TAG from wild type (*black bars*), TM *DGA1*$^+$ (*white bars*), and TM *LRO1*$^+$ (*gray bars*) strains. *B,* fatty acid analysis of SE from wild type (*black bars*), TM *ARE1*$^+$ (*white bars*), and TM *ARE2*$^+$ (*gray bars*) strains. Values are shown as percent of total fatty acids and are from three independent measurements with the respective mean deviation. *C16:0*, palmitic acid; *C16:1*, palmitoleic acid; *C18:0*, stearic acid; *C18:1*, oleic acid.

tribution of Are1p to total cellular SE formation was only minor compared with Are2p confirming previous results by others (20, 24, 37).

Interestingly, enzyme activities *in vitro* of the four different acyltransferases measured did not completely reflect the levels of products formed. Are1p and Are2p activities were measured with the same substrate in the same assay and exhibited the expected additive effect. In contrast, the activities of Dga1p and Lro1p were measured with different substrates and different assays and therefore could not be directly compared. Both enzyme activities were markedly decreased in mutant strains (Fig. 2). We have to take into account, however, that enzyme activities measured *in vitro* need not reflect the potential of an enzyme *in vivo*, but we also have to consider that changed cellular conditions in TM may be responsible for the observed alterations of the enzyme activities.

Neutral Lipid Product Profile Generated by Individual Acyltransferases—One explanation for the existence of TAG and SE synthases with overlapping function may be different substrate specificity and consequently formation of different product species. To address this question, we performed fatty acid and sterol analysis of TAG and SE formed by the respective individual acyltransferases.

The fatty acid composition of total lipids from the four different TM remained unchanged compared with wild type (data not shown). Thus, the overall cellular fatty acid formation was not affected by the absence of three neutral lipid-synthesizing acyltransferases. In contrast, the fatty acid composition of TAG and SE from the different TM varied compared with wild type. As can be seen from Fig. 3*A*, both the TM *DGA1*$^+$ and TM *LRO1*$^+$ strain contained more unsaturated fatty acids in the TAG fractions than wild type. This effect was mainly attributed to a shift from C-16:0 to C-16:1, but less from C-18:0 to C-18:1 species. These changes resulted in a marked alteration of the ratio of unsaturated to total fatty acids in TAG from TM *DGA1*$^+$ and TM *LRO1*$^+$ compared with wild type (Table 2). The ratio of C-16 to C-18 fatty acids was increased in TM *DGA1*$^+$ but unchanged in TM *LRO1*$^+$.

Fatty acid analysis of the SE fractions revealed that in TM *ARE1*$^+$ the amount of unsaturated fatty acids was slightly decreased compared with wild type (Fig. 3*B* and Table 2). No such effect was observed in the TM *ARE2*$^+$ strain, confirming that Are2p was the dominant SE synthase in the yeast. The ratio of C-16 to C-18 fatty acids in TM *ARE1*$^+$ was the same as in wild type and slightly increased in TM *ARE2*$^+$.

Similar to a certain specificity of neutral lipid synthesizing acyltransferases for fatty acids as substrates, Are1p and Are2p exhibited some preferences for sterol moieties incorporated into SE (Fig. 4). Zymosterol, fecosterol, lanosterol, and episterol are the four most abundant esterified sterols stored in the form of SE in LP both from TM *ARE1*$^+$ and TM *ARE2*$^+$. Whereas the sterol pattern of SE from TM *ARE2*$^+$ was almost identical to wild type, Are2p showed a slight preference for sterol precursors over ergosterol compared with wild type confirming previous results by Zweytick *et al.* (22) and Valachovic *et al.* (38). The sterol profile from whole TM cells, however, showed interesting differences between wild type and mutants, pointing to a regulatory effect of neutral lipid storage on sterol biosynthesis (Table 3). TM *DGA1*$^+$ and TM *LRO1*$^+$, which lacked sterol esterification, accumulated ergosta-7,22-dienol and ergosta-7-enol at the expense of other sterol precursors. This effect may be explained by down-regulation of Erg3p as reported previously by Arthington-Skaggs *et al.* (39) and will be discussed

TABLE 2

Fatty acid analysis of neutral lipids from wild type and strains bearing defects in neutral lipid synthesis

The ratios of unsaturated to total fatty acids (UFA/TFA) and ratio of 16 carbon chain to 18 carbon chain fatty acids (C16/C18) are shown. Data are mean values from three independent experiments with standard deviation. Strain genotypes are shown in Table 1.

Strain	UFA/TFA		C16/C18	
	TAG	SE	TAG	SE
W303 (wild type)	0.75 ± 0.06	0.90 ± 0.05	1.01 ± 0.22	0.74 ± 0.09
TM *DGA1*$^+$	0.91 ± 0.03		1.22 ± 0.27	
TM *LRO1*$^+$	0.90 ± 0.05		0.99 ± 0.16	
TM *ARE1*$^+$		0.72 ± 0.09		0.73 ± 0.09
TM *ARE2*$^+$		0.89 ± 0.07		0.82 ± 0.04

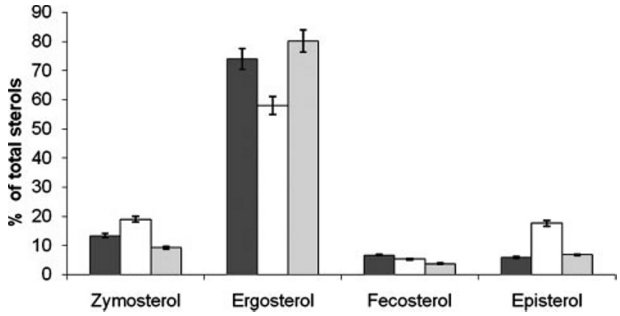


FIGURE 4. **Sterol composition of steryl esters from lipid particles.** The wild type W303 (*black bars*) and mutant strains TM *ARE1*$^+$ (*white bars*) and TM *ARE2*$^+$ (*gray bars*) were analyzed. Values are from three independent measurements and expressed as percent of total sterols.

below. Interestingly, the total amount of cellular sterols remained largely unchanged, which is at variance with earlier reports using an *are1*Δ*are2*Δ mutant strain (39). Yang *et al.* (20) reported that the concentration of free sterols in an *are1*Δ*are2*Δ mutant was similar to wild type. Zweytick *et al.* (22) showed that the level of total ergosterol in an *are1*Δ*are2*Δ mutant was slightly reduced compared with wild type. It has to be noted, however, that the values of wild type include amounts of free sterols and SE, whereas SE are missing in the double mutant. In TM *ARE1*$^+$ and TM *ARE2*$^+$ ergosta-7,22-dienol also accumulated to some extent, and also episterol and ergosta-7-enol levels were increased over wild type.

Electron Microscopic Inspection of Lipid Particle Variants—In the previous sections we described that TM lacking major enzymes of TAG or SE synthesis, respectively, form neutral lipids with very specific composition. Next, we asked whether or not such changes would affect the appearance and structure of LP. For this purpose, we analyzed TM whole cells to estimate size and shape of LP in these strains by electron microscopy. As can be seen from Fig. 5, all TM were able to form LP of comparable size and shape. Closer inspection of a statistically significant number of cells, however, revealed differences in the size distribution of LP from mutant strains (Fig. 6). Wild type LP exhibited a rather narrow size distribution with the maximum at a diameter of 350 and 450 nm. A large portion of LP from TM *LRO1*$^+$, TM *ARE1*$^+$, and TM *ARE2*$^+$, almost 40%, was 250–350 nm in diameter, but the maximum diameter was also 350–450 nm. In contrast, TM *DGA1*$^+$ showed a broader distribution of LP diameter with only ~25% in the range from 250 to 350 nm, but 30% in the range from 450–550 nm. Thus, the lipid composition of LP exhibited some effect on the size of this organelle.

Structural Studies with Isolated Lipid Particle Variants—For studies described in the following, highly purified LP from wild type and the different TM were required. Western blot analysis using antibodies against Erg1p, Por1p, Wbp1p, and Prc1p revealed that we were able to isolate LP from all strains used in this study with only a marginal degree of contamination (Fig. 7*A*). All LP preparations showed an appropriate enrichment of Erg1p over the homogenate and only minor signals from mitochondrial, ER, or vacuolar markers. Nevertheless, SDS-PAGE showed some marked differences of LP protein patterns from the different strains (Fig. 7*B*). Although individual proteins of the respective fractions were not analyzed in more detail, we can assume that changes in the lipid composition of LP also affected the protein equipment of these organelles, at least to some extent.

Isolated LP from wild type and TM were used in aqueous solution without further dilution for differential scanning calorimetry. Fig. 8 shows that upon heating, LP from wild type as well as from TM *ARE1*$^+$ and TM *ARE2*$^+$ exhibited two phase transitions, which differed in their enthalpies and transition temperatures (Table 4). In contrast, no such phase transition was detected with LP from TM *LRO1*$^+$ and TM *DGA1*$^+$ in the temperature range investigated (1–65 °C). This result, however, was not surprising, keeping in mind the chemical composition of the respective LP preparations and the molecules that may contribute to the observed transitions, namely SE, proteins, and phospholipids. The very small amount (2.6 and 1.3%, respectively) and the large variety of proteins and phospholipids present in LP, compared with 44.4% SE (1), made it unlikely that cooperative transitions were related to the melting of the phospholipid acyl chains and/or protein unfolding. This result is also in line with previous findings that no phase transition was detected for phospholipid monolayers in cholesterol-rich VLDL (CER-VLDL) or in LDL (40, 41). Therefore, the observed phase transitions in yeast LP were clearly because of the melting of acyl chains from SE. Most importantly, this view was confirmed by the observation that LP from TM *LRO1*$^+$ and TM *DGA1*$^+$ lacking SE did not exhibit any transition. Noteworthy, the transition enthalpy was about 1 order of magnitude lower in the wild type compared with TM *ARE1*$^+$ and TM *ARE2*$^+$. This result can be explained by the presence of TAG in LP from wild type, which is partially intercalated into SE-rich domains. Therefore, a disordering of the SE packing and consequently a decrease of the transition enthalpy were induced.

The two phase transitions observed in SE containing yeast LP (see Fig. 8) is reminiscent of the thermotropic behavior of pure cholesterol oleate, where transitions from smectic to cholesteric and from cholesteric to the liquid state occurred (41). A similar observation was reported for CER-VLDL and a respec-

TABLE 3

Whole cells sterol analysis from wild type and strains bearing defects in neutral lipid synthesis

Values are expressed as percent of total sterols with standard deviation. Data are mean values from three independent experiments. Strain genotypes are shown in Table 1. ND indicates not detectable.

	% of total sterols				
	W303	TM *DGA1*$^+$	TM *LRO1*$^+$	TM *ARE1*$^+$	TM *ARE2*$^+$
Ergosterol	71.3 ± 1.7	77.3 ± 0.3	78.2 ± 0.5	72.6 ± 0.4	79.7 ± 0.6
Zymosterol	10.6 ± 0.3	ND	ND	3.0 ± 0.4	7.5 ± 0.2
Ergosta-7,22-dienol	1.3 ± 0.2	8.6 ± 0.3	8.4 ± 1.1	5.7 ± 0.8	3.3 ± 0.2
Ergosta-5,7,22,24-tetraenol	3.1 ± 0.1	ND	ND	ND	2.0 ± 0.1
Fecosterol	4.4 ± 0.4	ND	ND	1.7 ± 0.1	4.5 ± 0.1
Episterol	5.8 ± 0.1	6.3 ± 0.6	4.9 ± 0.4	10.0 ± 0.4	9.2 ± 0.2
Ergosta-7-enol	ND	5.7 ± 0.4	4.9 ± 0.3	2.6 ± 0.1	1.7 ± 0.1
Lanosterol	1.7 ± 0.1	1.0 ± 0.1	1.6 ± 0.6	1.3 ± 0.2	1.0 ± 0.1
μg of total sterols/A_{600}	1.36 ± 0.18	1.44 ± 0.20	1.32 ± 0.21	1.49 ± 0.11	1.64 ± 0.10

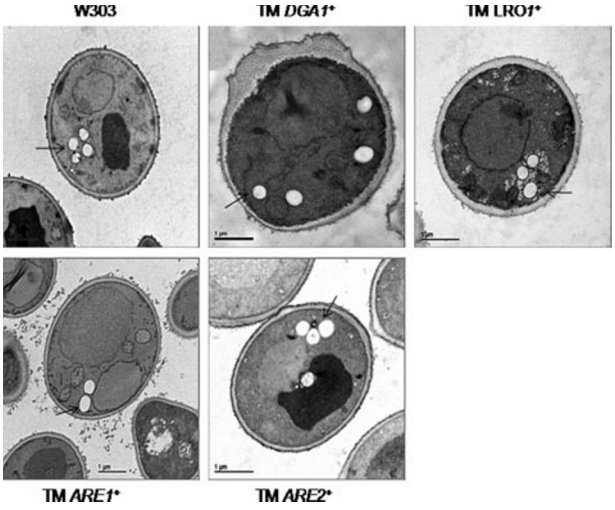


FIGURE 5. **Lipid particles in yeast mutants bearing defects in neutral lipid synthesis.** Electron micrographs of wild type W303 and mutant strains TM *DGA1*$^+$, TM *LRO1*$^+$, TM *ARE1*$^+$, and TM *ARE2*$^+$ were inspected as described under "Experimental Procedures." *Arrows* indicate LP structures in the different strains.

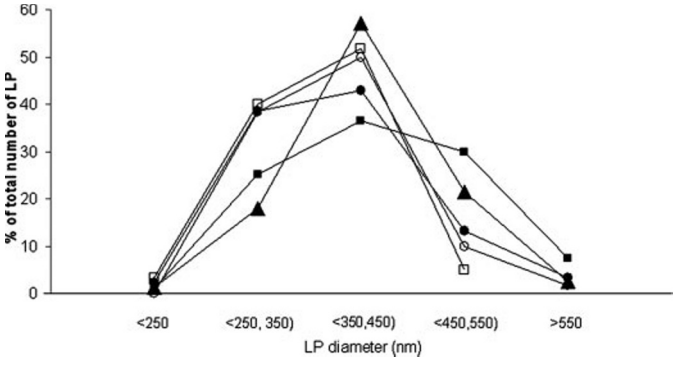


FIGURE 6. **Lipid particle size distribution.** The size of LP was estimated based on electron microscopic pictures (see "Experimental Procedures"). Data were main values from ~100 cells per strain. ▲, W303; ■,TM *DGA1*$^+$; □, TM *LRO1*$^+$; ●, TM *ARE1*$^+$; ○, TM *ARE2*$^+$.

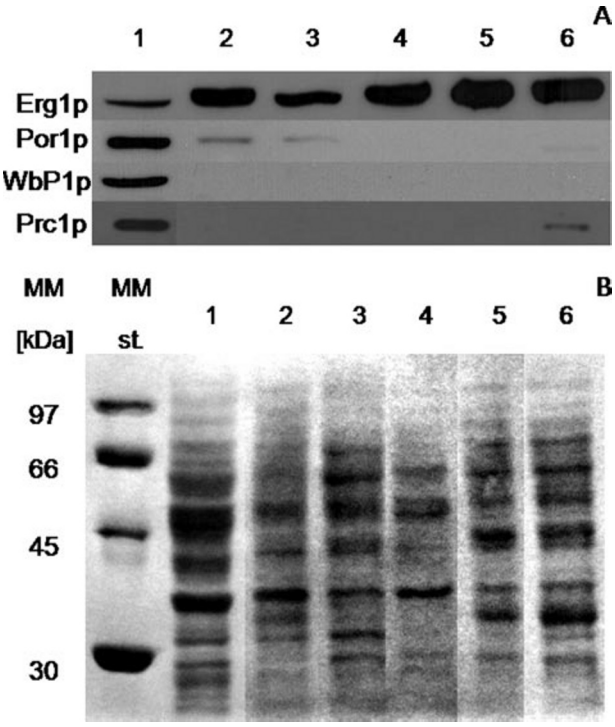


FIGURE 7. **Protein analysis of lipid particles from wild type and TM *LRO1*$^+$, TM *DGA1*$^+$, TM *ARE1*$^+$, and TM *ARE2*$^+$.** *A,* Western blot analysis using antibodies against Erg1p (LP marker), Por1p (mitochondrial marker), Wbp1p (microsomal), and Prc1p/CPY (vacuolar marker). *B,* SDS-PAGE. (*MM st.* = molecular mass standards). *Lane 1,* homogenate from wild type W303; *lane 2,* LP from wild type W303; *lane 3,* LP from TM *DGA1*$^+$; *lane 4,* LP from TM *LRO1*$^+$; *lane 5,* LP from TM *ARE1*$^+$; *lane 6,* LP from TM *ARE2*$^+$.

tive model mixture (40). These lipoprotein particles are characterized by a very low TAG content (~3%) and thus resemble LP from TM *ARE2*$^+$. Experiments with model systems showed that addition of 5% TAG can abolish the high temperature transition (41). Moreover, Pregetter *et al.* (42) showed that in human LDL at a CE to TAG ratio of 7:1 phase separation of a liquid TAG core and rigid shells of CE (radial ratio 2:1) occurred with an order-disorder transition temperature of 30 °C. Incorporation of further TAG led to a decrease of this phase transition as also observed with yeast wild type LP (see Fig. 8). In contrast to wild type, LP from TM *ARE1*$^+$ and TM *ARE2*$^+$ contain a larger fraction of SE layers in an ordered state at physiological temperature.

To obtain more structural information about yeast LP, small-angle x-ray scattering experiments were performed using LP preparations from wild type and TM *ARE2*$^+$ at temperatures below, between, and above the two phase transitions that had been identified by DSC. It has to be noted that the weak intensity of Bragg peaks and the high background noise are because of the low sample concentration that could not be enhanced despite various experimental efforts. Both samples exhibited diffuse particle scattering over the whole temperature range measured (data not shown). Additionally, at 1 °C (below

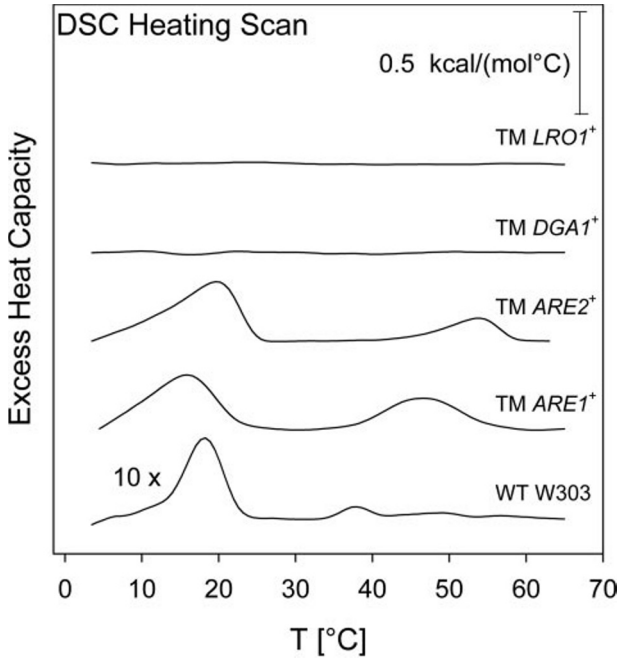


FIGURE 8. **Differential scanning calorimetry thermograms of lipid particle preparations from wild type, TM *ARE1*$^+$, TM *ARE2*$^+$, TM *DGA1*$^+$, and TM *LRO1*$^+$ strains.** A comparison of heating scans of LP preparations from wild type W303 and TM strains is shown as indicated in the panel. The thermograms showing the second heating scan after one heating-cooling cycle are displaced for clarity on the *y* axis by arbitrary units, and the excess heat capacity profile of the wild type is enlarged by a factor of 10. The scan rate was 15 °C/h.

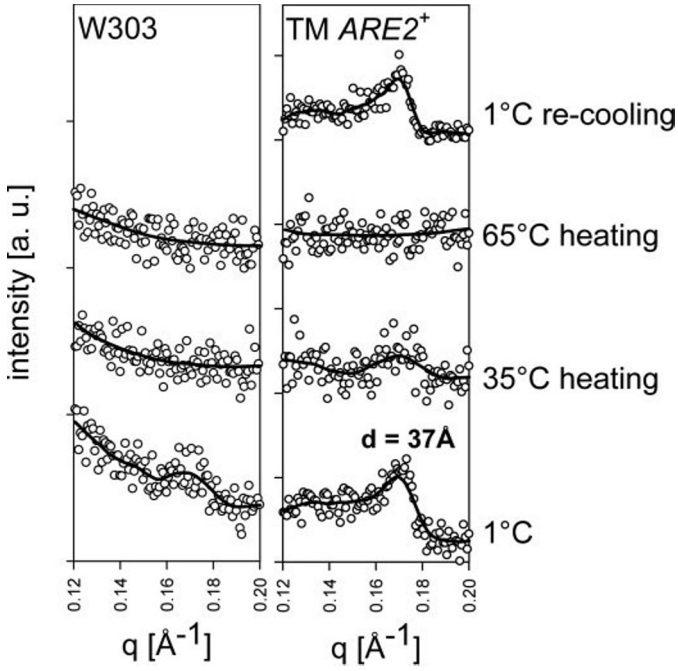


FIGURE 9. **Small x-ray scattering pattern of lipid particle preparations from wild type W303 and TM *ARE2*$^+$.** Temperatures are indicated in the panel. Offsets have been added to shift the data vertically; $q = 4\pi\sin\theta/\lambda$ is the scattering vector. *Open circles* are the experimental data; *solid lines* show smoothened data to guide the eye.

TABLE 4

Thermodynamic parameters of lipid particles from *S. cerevisiae* wild type W303, and TM with only Are1p or Are2p, respectively, active

T_{m1}, low temperature transition; T_{m2}, high temperature transition; $\Delta H_{cal,1}$, enthalpy of low temperature transition; $\Delta H_{cal,2}$, enthalpy of high temperature transition.

Strain	T_{m1}	$\Delta H_{cal,1}$	$T_{m,2}$	$\Delta H_{cal,2}$
	°C	*kcal/mol*	°C	*kcal/mol*
W303 (wild type)	18.1	0.32	38.0	0.06
TM *ARE1*$^+$	16.5	2.25	46.6	1.70
TM *ARE2*$^+$	20.2	3.20	54.0	1.00

T_{m1}), a weak Bragg reflection with a maximum at $q \sim 0.17$ Å^{-1} was observed, which was more pronounced for TM *ARE2*$^+$ than wild type. This result reflected the higher amount of rigid SE/protein in the TM *ARE2*$^+$ than in the wild type. It was in accordance with the lower enthalpy of this transition observed for the wild type (see above). LP from TM *ARE2*$^+$ (Fig. 9) still showed an even broader Bragg reflection at 35 °C with decreased intensity and complete loss at 65 °C, which is in agreement with the chain melting behavior observed by DSC revealing a second phase transition between 35 and 65 °C. Most importantly, upon re-cooling, the Bragg reflection re-occurred at the same position indicating reversibility of the structural alterations and arguing against an artifact created by low temperature. This result parallels DSC, which also showed complete reversibility of phase transitions during repeated heating and cooling experiments. It has to be noted that Fig. 8 shows the second heating scan after one heating-cooling cycle. Interestingly, the position of the Bragg peak relating to a repeat distance of about 37 Å is close to 36 Å, the value reported for cholesteryl ester shells (43). A similar Bragg peak position was reported for the human LDL particles indicating the smectic-like liquid-crystalline phase of CE, which also disappeared above the phase transition temperature (43–46). Taken together, these results suggest a shell-like arrangement of SE also within the yeast LP as was postulated before for the CER-VLDL (40). No Bragg peak was observed in SAXS patterns using LP from TM *LRO1*$^+$ and TM *DGA1*$^+$ (data not shown), which was not surprising because these strains lack SE. One has to assume that in these LP variants only the surface phospholipid monolayer with embedded proteins protects the fluid TAG core from the aqueous environment.

DISCUSSION

During the last few years evidence accumulated suggesting that LP from the yeast as well as from other cell types do not only serve as a lipid storage compartment but also fulfill a number of other functions. As an example, it has been shown that LP harbor specific enzymes mainly involved in lipid metabolism (for reviews see Refs. 7, 10) and thus contribute actively to the formation of cellular components. Neutral lipids of LP from *S. cerevisiae* have also been shown to be involved in protein stabilization as demonstrated for Erg1p (8). An additional process affected by the lack of neutral lipids is yeast spore formation (11). Moreover, lack of TAG synthesis in *Schizosaccharomyces pombe* was proposed to lead to apoptosis (47) when the protective role of TAG as an inert storage depot for bioactive molecules like diacylglycerol and fatty acids was missing. Finally, a potential role of LP in sequestering toxic hydrophobic components from the rest of the cell and protecting the cell from

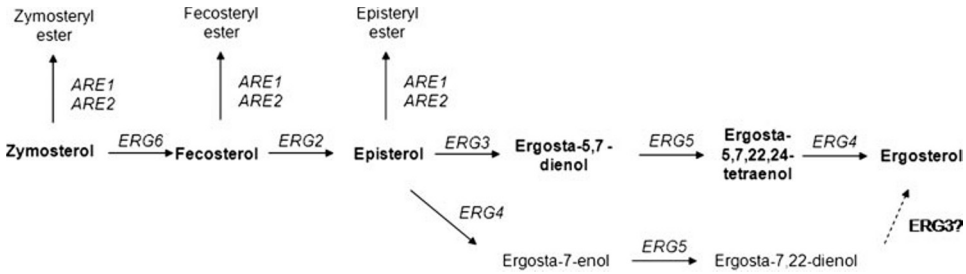


FIGURE 10. **Effect of sterol esterification on sterol biosynthesis.** Lack of sterol esterification down-regulates Erg3p (39), which causes a decreased amount of ergosta-5,7,22,24-tetraenol and an increased amount of ergosta-7-enol and ergosta-7,22-dienol. This effect may pave the way for an alternative pathway of episterol conversion by Erg4p and Erg5p to ergosterol.

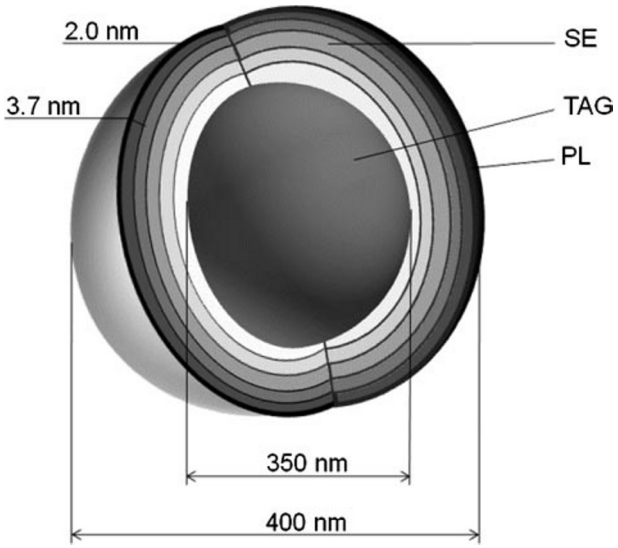


FIGURE 11. **Model of a yeast lipid particle.** TAG form the inner core of LP, which is surrounded by shells consisting of SE most likely with some TAG intercalated. For the sake of clarity the shells were oversized compared with the TAG core. The thickness of SE shells is 3.7 nm. A PL monolayer forms the surface of LP.

lipotoxicity has also been discussed. Indeed, yeast cells lacking LP were shown to be highly sensitive to oleate (48).[4]

In this study, we demonstrate that LPs are highly dynamic and flexible organelles. As shown under "Results," deletion of three of four acyltransferases involved in neutral lipid synthesis of *S. cerevisiae* led to dramatic changes in the lipid profile of LP. Depending on the remaining acyltransferase in TM, Dga1p, Lro1p, Are1p, or Are2p, respectively, the neutral lipid pattern of these strains was restricted to either TAG or SE. Moreover, moderate changes in the fatty acid composition of TAG and SE from TM were found (see Fig. 3) suggesting different substrate specificities of these acyltransferases. Sandager *et al.* (37) reported that in strains lacking Dga1p, marked amounts of vaccenic acid and palmitoleic acid accumulated. The reason for these changes was unclear, but it was assumed that eliminating acyl-CoA-dependent TAG synthesis affected size and composition of acyl-CoA pools and thus the cellular fatty acid composition.

More dramatic changes were observed in the sterol profile of the SE fraction and total lipids from TM. TM *ARE1*$^+$ contained more than 40% of ergosterol precursors in the SE fraction compared with 25 and 20% in wild type and TM *ARE2*$^+$, respectively. These variations can at least in part be explained by substrate specificities of Are1p and Are2p confirming previous data by Zweytick *et al.* (22) and Valachovic *et al.* (24). In contrast, changes in the sterol composition of TM *DGA1*$^+$ and TM *LRO1*$^+$ cannot be attributed to substrate specificities of (missing) SE synthases but rather to a feedback regulation to the sterol biosynthetic pathway. This view is in line with data reported by Arthington-Skaggs *et al.* (39) showing that lack of Are1p or Are2p down-regulated Erg3p. This down-regulation may be the reason for the accumulation of ergosta-7-enol and ergosta-7,22-dienol (Fig. 9) observed in all TM but especially in TM *DGA1*$^+$ and TM *LRO1*$^+$. Besides the normal pathway of desaturation to ergosta-5,7-dienol and further to ergosta-5,7,22,24-tetraenol, in these strains a marked portion of episterol seems to be converted to ergosta-7-enol by Erg4p and subsequently to ergosta-5,7-dienol by Erg5p. The last step of the ergosterol biosynthesis may be accomplished by residual Erg3p. Another interesting change in sterol metabolism is the absence of zymosterol and fecosterol in TM *DGA1*$^+$ and TM *LRO1*$^+$ (see Table 3). We assume that these two precursors are esterified with some preference in the presence of Are proteins and thus partially channeled away from the main ergosterol synthesis pathway. Because of the inability of TM *DGA1*$^+$ and TM *LRO1*$^+$ to esterify zymosterol and fecosterol, these sterol intermediates appear to be readily converted to episterol and further to ergosterol (see Fig. 10). Thus, the presence or absence of sterol esterification has a marked influence on the cellular sterol profile.

Despite all changes in the neutral lipid profile, LP were readily generated in all TM although at some variance. Electron microscopy revealed some differences in the size distribution of LP from TM with the most pronounced effect in TM *DGA1*$^+$ showing a marked portion of LP with a diameter that is significantly higher than in wild type. Dynamic light scattering measurements confirmed the size distribution of LP measured by microscopy (data not shown). Dga1p is the only one of the four acyltransferases involved in neutral lipid synthesis that is dually localized to LP and the ER (19), and it appears to be mainly involved in TAG synthesis in the stationary growth phase (9). Thus, Dga1p may be responsible for increasing the amount of TAG *in situ* in existing LP and for the larger size of LP in TM *DGA1*$^+$.

LP variants produced in the different TM described in this study enabled us to perform structural analysis of this organelle. According to data derived from biophysical and biochemical investigations, a model for the inner structure of wild type LP was established (Fig. 11). Differential scanning calorimetry and x-ray analyses suggested that LP contain rigidly packed shells of SE that become fluid-like at certain transition temperatures. Reversibility of the structural changes upon heating and cooling confirmed the relevance of the proposed structure also under physiological conditions. The low enthalpy of these transitions (DSC) and the low intensity of the Bragg peak (x-ray) indicated

[4] M. Connerth, unpublished results.

that not all SE in LP were in an ordered state but perturbed by intercalated TAG. In analogy to models proposed for CER-VLDL (40) and human LDL (43–46), which suggested rigid packing of CE at low temperature with long molecular axes arranged in concentric shells of ~36 Å radii, a shell-like arrangement of SE can also be postulated for yeast LP. Calculations based on lipid quantification and hydrophobic volumes of TAG and SE suggested that the TAG core of yeast LP was surrounded by a maximum of 10 shells of SE. Previously, it has already been shown that a phospholipid monolayer of ~2 nm with proteins embedded formed the surface of yeast LP (1).

LP from TM *ARE2*$^+$ appeared to be differently structured, namely similar to CER-VLDL which are also very poor in TAG and in the size range of yeast LP. We assume that in this LP variant the absence of TAG leads to a higher ordered structure in the particle below the phase transition with a larger number of concentric SE layers being also present at physiological temperature, which may be relevant for SE mobilizations in these mutants.

The structural model of yeast LP proposed here may explain some physiological properties of this organelle. Rigid shells of SE existing at the physiological temperature may influence the metabolic behavior of LP and protect the inner core of TAG being degraded in an uncontrolled way by TAG lipases present in the surface monolayer of LP. SE in an ordered state appear to give the LP some stability. It has to be taken into account, however, that under laboratory conditions LP are in a nearly completely disordered state with TAG and SE largely exposed to TAG lipases and SE hydrolases. This is actually one of the important questions related to balanced neutral lipid storage and mobilization. It will be a task for the future to investigate how TAG lipases and SE hydrolases get access to their substrates stored in LP. Surface structure analysis and especially topological analysis of neutral lipid hydrolytic enzymes on the LP surface will contribute to a better understanding of this problem.

Acknowledgments—We thank Sten Stymne for providing yeast mutant strains and Harald Pichler for help interpreting the GLC/MS. We thank Ruth Prassl and Peter Laggner for discussions of the biophysical data.

REFERENCES

1. Leber, R., Zinser, E., Zellnig, G., Paltauf, F., and Daum, G. (1994) *Yeast* **10,** 1421–1428
2. Athenstaedt, K., Zweytick, D., Jandrositz, A., Kohlwein, S. D., and Daum, G. (1999) *J. Bacteriol.* **181,** 6441–6448
3. Athenstaedt, K., and Daum, G. (1999) *Eur. J. Biochem.* **266,** 1–16
4. Johnson, D. R., Knoll, L. J., Levin, D. E., and Gordon, J. I. (1994) *J. Cell Biol.* **127,** 751–762
5. Duronio, R. J., Knoll, L. J., and Gordon, J. I. (1992) *J. Cell Biol.* **117,** 515–529
6. Watkins, P. A., Lu, J. F., Steinberg, S. J., Gould, S. J., Smith, K. D., and Braiterman, L. T. (1998) *J. Biol. Chem.* **273,** 18210–18219
7. Zinser, E., Paltauf, F., and Daum, G. (1993) *J. Bacteriol.* **175,** 2853–2858
8. Sorger, D., Athenstaedt, K., Hrastnik, C., and Daum, G. (2004) *J. Biol. Chem.* **279,** 31190–31196
9. Oelkers, P., Cromley, D., Padamsee, M., Billheimer, J. T., and Sturley, S. L. (2002) *J. Biol. Chem.* **277,** 8877–8881
10. Athenstaedt, K., and Daum, G. (2003) *J. Biol. Chem.* **278,** 23317–23323
11. Athenstaedt, K., and Daum, G. (2005) *J. Biol. Chem.* **280,** 37301–37309
12. Mullner, H., Deutsch, G., Leitner, E., Ingolic, E., and Daum, G. (2005) *J. Biol. Chem.* **280,** 13321–13328
13. Koffel, R., Tiwari, R., Falquet, L., and Schneiter, R. (2005) *Mol. Cell. Biol.* **25,** 1655–1668
14. Jandrositz, A., Petschnigg, J., Zimmermann, R., Natter, K., Scholze, H., Hermetter, A., Kohlwein, S. D., and Leber, R. (2005) *Biochim. Biophys. Acta* **1735,** 50–58
15. Czabany, T., Athenstaedt, K., and Daum, G. (2007) *Biochim. Biophys. Acta* **1771,** 299–309
16. Oelkers, P., and Sturley, S. L. (2004) in *Lipid Metabolism and Membrane Biogenesis* (Daum, G., ed) pp. 289–311, Springer-Verlag, Berlin
17. Oelkers, P., Tinkelenberg, A., Erdeniz, N., Cromley, D., Billheimer, J. T., and Sturley, S. L. (2000) *J. Biol. Chem.* **275,** 15609–15612
18. Dahlqvist, A., Stahl, U., Lenman, M., Banas, A., Lee, M., Sandager, L., Ronne, H., and Stymne, S. (2000) *Proc. Natl. Acad. Sci. U. S. A.* **97,** 6487–6492
19. Sorger, D., and Daum, G. (2002) *J. Bacteriol.* **184,** 519–524
20. Yang, H., Bard, M., Bruner, D. A., Gleeson, A., Deckelbaum, R. J., Aljinovic, G., Pohl, T. M., Rothstein, R., and Sturley, S. L. (1996) *Science* **272,** 1353–1356
21. Yu, C., Kennedy, N. J., Chang, C. Y., and Rothblatt, J. A. (1996) *J. Biol. Chem.* **271,** 24157–24163
22. Zweytick, D., Leitner, E., Kohlwein, S. D., Yu, C., Rothblatt, J., and Daum, G. (2000) *Eur. J. Biochem.* **267,** 1075–1082
23. Jensen-Pergakes, K., Guo, Z., Giattina, M., Sturley, S. L., and Bard, M. (2001) *J. Bacteriol.* **183,** 4950–4957
24. Valachovic, M., Klobucnikova, V., Griac, P., and Hapala, I. (2002) *FEMS Microbiol. Lett.* **206,** 121–125
25. Tinkelenberg, A. H., Liu, Y., Alcantara, F., Khan, S., Guo, Z., Bard, M., and Sturley, S. L. (2000) *J. Biol. Chem.* **275,** 40667–40670
26. Kurat, C. F., Natter, K., Petschnigg, J., Wolinski, H., Scheuringer, K., Scholz, H., Zimmermann, R., Leber, R., Zechner, R., and Kohlwein, S. D. (2006) *J. Biol. Chem.* **281,** 491–500
27. Koffel, R., and Schneiter, R. (2006) *Eukaryot. Cell* **5,** 1018–1025
28. Zinser, E., and Daum, G. (1995) *Yeast* **11,** 493–536
29. Lowry, O. H., Rosebrough, N. J., Farr, A. L., and Randall, R. J. (1951) *J. Biol. Chem.* **193,** 265–275
30. Laemmli, U. K. (1970) *Nature* **227,** 680–685
31. Haid, A., and Suissa, M. (1983) *Methods Mol. Biol.* **96,** 192–205
32. Folch, J., Lees, M., and Sloane-Stanley, G. H. (1957) *J. Biol. Chem.* **226,** 497–509
33. Morrison, W., and Smith, L. (1964) *J. Lipid Res.* **5,** 600–608
34. Quail, M. A., and Kelly, S. L. (1996) *Methods Mol. Biol.* **53,** 123–131
35. Yang, H., Cromley, D., Wang, H., Billheimer, J. T., and Sturley, S. L. (1997) *J. Biol. Chem.* **272,** 3980–3985
36. Reynolds, E. S. (1963) *J. Cell Biol.* **17,** 208–212
37. Sandager, L., Gustavsson, M. H., Stahl, U., Dahlqvist, A., Wiberg, E., Banas, A., Lenman, M., Ronne, H., and Stymne, S. (2002) *J. Biol. Chem.* **277,** 6478–6482
38. Valachovic, M., Hronska, L., and Hapala, I. (2001) *FEMS Microbiol. Lett.* **197,** 41–45
39. Arthington-Skaggs, B. A., Crowell, D. N., Yang, H., Sturley, S. L., and Bard, M. (1996) *FEBS Lett.* **392,** 161–165
40. Morrisett, J. D., Gaubatz, J. W., Tarver, A. P., Allen, J. K., Pownall, H. J., Laggner, P., and Hamilton J. A. (1984) *Biochemistry* **23,** 5343–5352
41. Kroon, P. A. (1981) *J. Biol. Chem.* **256,** 5332–5339
42. Pregetter, M., Prassl, R., Schuster, B., Kriechbaum, M., Nigon, F., Chapman, J., and Laggner, P. (1999) *J. Biol. Chem.* **274,** 1334–1341
43. Deckelbaum, R. J., Shipley, G. G., Small, D. M., Lees, R. S., and George, P. K. (1975) *Science* **190,** 392–394
44. Deckelbaum, R. J., Shipley, G. G., and Small, D. M. (1977) *J. Biol. Chem.* **252,** 744–754
45. Laggner, P., Degovics, G., Muller, K. W., Glatter, O., Kratky, O., Kostner, G., and Holasek, A. (1977) *Hoppe-Seyler's Z. Physiol. Chem.* **358,** 771–778
46. Atkinson, D., Deckelbaum, R. J., Small, D. M., and Shipley, G. G. (1977) *Proc. Natl. Acad. Sci. U. S. A.* **74,** 1042–1046
47. Low, C. P., Liew, L. P., Pervaiz, S., and Yang, H. (2005) *FEMS Yeast Res.* **5,** 1199–1206
48. Lockshon, D., Surface, L. E., Kerr, E. O., Kaeberlein, M., and Kennedy, B. K. (2007) *Genetics* **175,** 77–91